ABERRATIONS REDUCTION IN DEFLECTING RF STRUCTURES FOR TRANSFORMATION OF PARTICLE DISTRIBUTION IN THE BUNCH

V. Paramonov, P. Orlov, K. Floettmann***
*INR of the RAS; *MPhTI, Moscow, Russia;*
***DESY, Hamburg, Germany*
E-mail: paramono@inr.ru

The complete analysis of field distribution in the deflecting RF structures (DS) has been performed and criterion for selection and development of DS with reduced aberrations is developed. Additional reasons to possible increasing of aberrations in DS sections are considered and difference between traveling and standing modes is outlined. Distortions of DS dispersion curve, coming with aberrations reduction, are considered and method for correction is applied. Examples of DS with the reduced level of aberrations are considered shortly.

PACS: 29.27.-a; 41.85.-p

The DS – periodical structures with transverse components of the electromagnetic field at the axis – were introduced initially for charged particle deflection and separation. A bunch of charged particles crosses a DS synchronously with the maximal deflecting field E_d, corresponding to a phase ϕ=0 in the structure, and all particles get an increment in the transverse momentum p_t. It allows both to deflect particles from the axis and to separate particles with different charge and momentum in space. In the modern facilities with short and bright bunches DS found other applications, such as short bunch rotation for special diagnostics [1], emittance exchange experiments and luminosity enhancement. All these applications are related to the Transformation of Particle Distributions (TPD) in the six dimensional phase space. For TPD the DS operates in another mode – the center of the bunch crosses the DS at zero value of E_d, corresponding to ϕ=90°, Fig. 1.

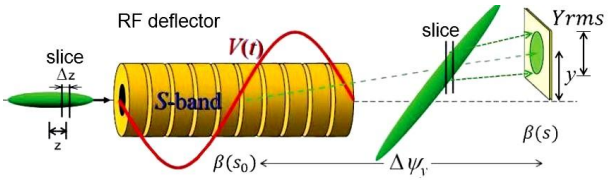

Fig. 1. The bunch rotation with DS for measurements of longitudinal distributions, [1]

The applications for particle distribution transformations provide additional specific requirements. Together with the expected transformations, DS provide distortions, due to particularities in the deflecting field distribution - aberrations, generated by nonlinear additions in the field distribution, caused by higher spatial harmonics and another reasons. The tool for TPD should provide as minimal as possible intrinsic distortions [2].

As it is known from theory, a system with linear spatial distribution of the field components doesn't change the bunch emittance. In this report we investigate DS's options for criteria of field linearity, i.e. minimal deviations from a linear field distribution – minimal level of aberrations.

1. FIELD DESCRIPTION AND ANALYSIS

For E_d description the widely used basis of *TM* - *TE* waves can not be used due to degeneration into *TEM* at particle velocity β_p=1. A basis of hybrid waves *HE* - *HM* waves was introduced, [3, 4] to avoid this methodical problem. The common representation for the field distribution in the DS aperture is

$$\vec{E} = A\vec{E}_{HE} + B\vec{E}_{HM}, \quad (1)$$

where the weighting coefficients *A,B* depend both on supporting structure and on operating mode. The deflecting field is derived from the transverse component of the Lorenz force

$$\vec{F}_L = e(\vec{E} + [\vec{v}, \vec{B}]), F_x = eE_d = e(E_x - \beta_p Z_0 H_y), Z_0 = \sqrt{\frac{\mu_0}{\varepsilon_0}} \quad (2)$$

and is expressed in (2) through the transverse field components E_x and H_y in the Cartesian coordinates.

In any periodical DS for Traveling Wave (TW) operating mode each field component $E_j(r,z)$ in the beam aperture, including also $E_d(r,z)$, can be represented in the complex form as the set over spatial harmonics:

$$E_j(r,z) = \hat{E}_j(r,z)e^{i\psi_j(z)} = \sum_{n\to-\infty}^{n\to\infty} a_{jn}(r)e^{-ik_{zn}z}, k_{zn} = \frac{\theta + 2n\pi}{d_p}, \quad (3)$$

with amplitude and phase $\psi_j(z)$ distribution. The period length d_p is normally matched of the particle β_p and the main spatial harmonic in (3) with the phase velocity β_0 as d_p = (θβλ)/(2π), where θ and λ are the operating phase advance and wavelength.

As it was shown in [3, 4], for the main spatial harmonics both for HE and HM waves for relativistic case β_0 the deflecting field is free from aberrations,

$$F_x(z) = e \cdot E_d = const, F_y(z) = 0. \quad (4)$$

For the Disk Loaded Waveguide (DLW) the well known expressions for field components were obtained, see, for example [5], in the small pitch approximation, which neglects all higher spatial harmonics, $\beta_0 = \beta_p$=1, $d_p << \lambda$, t << d_p.. But the total deflecting field is not only main spatial harmonics. More detailed general analysis [6] of the field distribution near axis revealed three reasons for nonlinear additions in periodical DS.

The first addition arises only in DS with a period length matched to the particle velocity $\beta_p=\beta_0$ <1. A simple expansion for the distribution of the fundamental harmonics leads to a description as:

$$F_x(z) \approx \frac{e(a_0 k_{zo} - b_0 k)}{2k_{z0}}(1 + k_{s0}^2 \frac{x^2 + y^2}{4} + \ldots),$$
$$F_y(z) \approx \frac{e(a_0 k_{zo} - b_0 k)}{2k_{z0}}(k_{s0}^4 (x^3 y + xy^3) + \ldots), \quad (5)$$
$$k = \frac{2\pi}{\lambda}, k_{s0}^2 = \left| k^2 - k_{z0}^2 \right|.$$

In the non-relativistic case already the field of the main harmonics is not free of nonlinear additions. The aberrations are important for low particle energy and vanish with $1/(\beta^2\gamma^2)$ for higher energies.

The second addition is the main source for transverse nonlinearities and arises from higher spatial harmonics. The effective deflecting force of the *n*-th harmonic is:

$$F_x(z) \approx \frac{e k_{sn}(a_n + b_n)}{2k_{z0}}(1 + k_{sn}^2 \frac{x^2 + y^2}{4} + \ldots) e_{zn},$$
$$F_y(z) \approx \frac{e k_{sn}(a_n + b_n)}{2k_{z0}}(k_{sn}^4 (x^3 y + xy^3) + \ldots) e_{zn}, \quad (6)$$
$$k_{sn}^2 = \left| k^2 - k_{zn}^2 \right|,$$

where e_{zn} is the corresponding harmonic in E_z component.

The third addition arises due to a break of the rotational symmetry of the DS, which is either a feature of the original DS design or which needs to be introduced in order to define the direction of the deflecting field. The nearest component has a sextupole wave structure, and the transverse force even of the main harmonic is:

$$F_x(z) \sim const \cdot k^2 (x^2 - y^2), F_y(z) \sim const \cdot 2k^2 xy. \quad (7)$$

2. ABERRATIONS REDUCTION

Aberrations due to the non-relativistic case, (5), are inevitable. Multipole additions, sextupole (7) and higher, should be minimized specially in the DS design, similar to [7]. The main attention has been paid to reduction of higher spatial harmonics in deflecting field of the dipole mode.

To estimate field quality, we have to estimate the level of spatial harmonics. For each harmonic the transverse and longitudinal distributions are rigidly coupled and are proportional to harmonic amplitude. Spatial harmonics are essential at the aperture radius $r=a$ and higher harmonics attenuate to the axis as

$$a_{jn}(0) \sim a_{jn}(a) \cdot \exp(-\frac{4\pi n}{\beta\theta} \cdot \frac{a}{\lambda}), |n| > 1. \quad (8)$$

At the DS axis r=0 just lower harmonics are really presented. For harmonics estimations at the axis in details and 'in total', we introduce parameters $\delta\psi_j(z)$ and Ψ_j as

$$\delta\psi_j(z) = \psi_j(z) + k_{z0} z, \Psi_j = \max(\left|\delta\psi(z)\right|),$$
$$0 \le z \le d_p, r = 0, \quad (9)$$

with the physical sense of the deviation and the maximal deviation of the phase of the total field component in (3) from the phase of synchronous harmonic, see [6] for more explanations and details. All time smaller Ψ_d value corresponds to lover level of higher spatial harmonics in E_d and vice versa. The value Ψ_d depends on DS design and operating value θ.

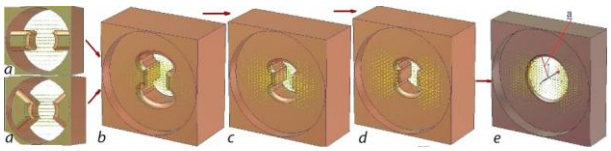

Fig. 2. Possible DS transformation

There is a large variety of RF structures with transverse fields, which can be used for deflection. For example, in Fig. 2 is shown a possible line of DS geometrical transformation. Instead of transformation looks more or less continuous, structures in Fig. 2,a,b and Fig. 2,d,e have quite different quality of E_d distribution.

2.1. TRAVELING WAVE OPERATION

In Fig. 3 are shown the surfaces $\Psi_z(a,\theta)$ for the original field component E_z and $\Psi_d(a,\theta)$ for E_d, which is composed, (2), from two components of the original field.

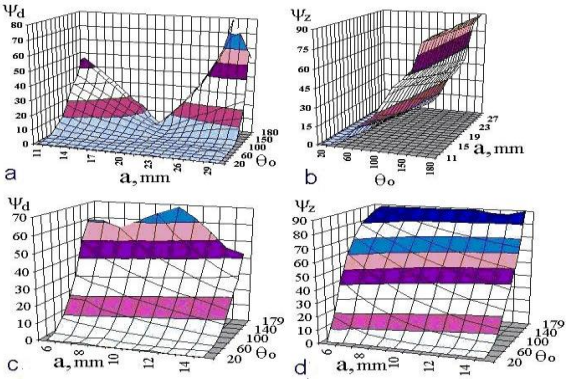

Fig. 3. The surfaces $\Psi_d(a, \theta)$, (a, c), and $\Psi_z(a, \theta)$, (b, d) for the DLW (a, b), Fig. 2,e and TE-type (c ,d), Fig. 2,b, DS's, λ=10 cm

The effect of higher spatial harmonics attenuation (8) is common for all periodical structures, and for low θ values one can see in Fig. 2 low $\Psi_z(a, \theta)$ and $\Psi_d(a, \theta)$ values for both structures. Nonlinear additions in the deflecting force are hence reduced in DS with large apertures, operating in TW mode with $\theta << 180°$.

But more generally is the importance of mutual phasing of hybrid waves *HE* and *HM* in (1). As one can see from (6), the contribution of the *n*-th harmonic in E_d vanishes if $a_n \sim - b_n$, regardless to the amplitude of corresponding harmonic e_{zn} in original field. For opposite phasing of the hybrid waves *HE* and *HM*, i.e. $A*B < 0$ in (1), the higher spatial harmonic of the electric field E_x partially compensate the corresponding harmonic of the magnetic field H_y, while for equal phasing $A*B > 0$ the amplitude of the deflecting force of the *n*-th harmonic is even larger than the amplitudes of the corresponding field components.

The DLW structure in the first passband has the opposite phasing and one can see in Fig. 3 the slower $\Psi_d(a,\theta)$ rise with θ, as compared to corresponding $\Psi_z(a,\theta)$ rise. Also the is the clear canyon in $\Psi_d(a,\theta)$ surface (see Fig. 3,a), corresponding to the curve a(θ), which provides condition $A \sim -B$. The TE-structure [7] has the equal phasing and one can see in Fig. 3 the faster $\Psi_d(a,\theta)$ rise with θ, as compared to corresponding $\Psi_z(a,\theta)$ rise and no minimum in $\Psi_d(a,\theta)$ surface.

The classification of a DS with a complicated field distribution is always rather conditional and visual defi-

nition of hybrid waves phasing is not evident. In [6] shown, that DS with a pronounced predominance of the transverse electric field in the aperture $|E_x| >> |E_z|$ ensue an equal phasing of the hybrid waves.

In Fig. 4,a are shown the plots of E_d and E_z distributions for a DLW in TW mode with θ=120°, which is similar to well known LOLA structures, [8]. The ripple in distributions is due to higher spatial harmonics. Similar plots are shown in Fig. 4,b for with θ=60° and more balanced ratio of hybrid waves. According simulations [2], the higher spatial harmonics for θ=60° are reduced ~40 times in E_z and ~ 3.5 times in E_d. The beam dynamics simulations through the structures was performed with the program ASTRA [9], showing ~ 2 times less growth of the transverse emittance in the direction of deflection for θ=60°

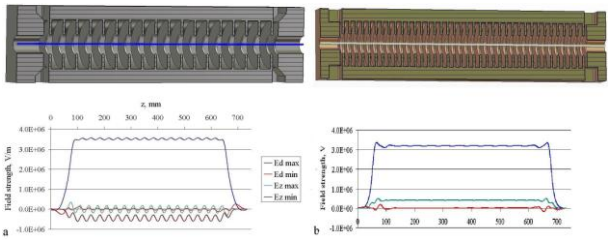

Fig. 4. Plots of E_d and E_z distributions for a DLW in TW mode, θ=120° (a) and θ=60° (b). The plots colors are – E_d, ϕ=0° – blue, E_d, ϕ=90° – red and E_d, ϕ=90° brown (a) and green (b)

At present time the DLW structure in TW mode with θ~60° in the field distribution quality looks the best for *6D* PDT.

2.2. STANDING WAVE OPERATION

For the Standing Wave (SW) operating mode, θ=180°, the natural harmonics attenuation (8) is not effective and the opposite phasing of the hybrid waves *HE* and *HM* together with balancing *A* ~ *-B* becomes the single way for aberrations reduction, more important than for TW case.

Even considering only the main n=0 harmonics in E_x and H_y field components, for the synchronous E_d harmonic in SW mode one has, [6]:

$$E_{d0} = e_{x0}\cos(kz+\phi)\cos(kz) - Z_0 h_{y0} sin(kz+\phi)\sin(kz) = \\ = \frac{e_{x0} - Z_0 h_{y0}}{2}\cdot\cos(\phi) + \frac{e_{x0} + Z_0 h_{y0}}{2}\cdot\cos(2kz+\phi). \quad (10)$$

For any initial phase shift ϕ the central particle sees both a uniform and an oscillating impact of the deflecting field. Even if the main harmonics are free from aberrations, the oscillating part in (10) shifts the particles bunch as the whole from the DS axis to regions with higher field nonlinearities from the higher spatial harmonics. As one can see from (10), the ratio of uniform and oscillating parts depends on the phasing and the balance of the hybrid waves *HE* and *HM*.

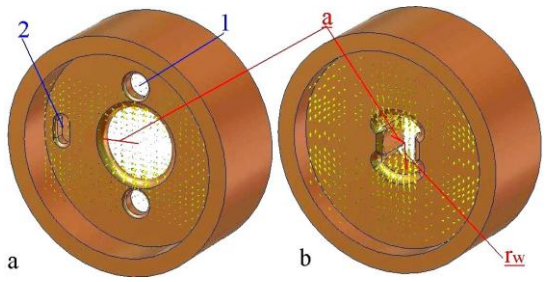

Fig. 5. SW structures with the minimized E_d aberrations, the optimized DLW structure (a) with holes for the deflecting plane stabilization (1) and slots for dispersion correction (2), and the decoupled structure (b)

For the SW case the parameter $\Psi_d(a,180°)$ works only for E_d field with the opposite phasing of the hybrid waves *HE* and *HM* for minimization of oscillating terms 'in total', [6]. The further study [10] was concentrated for the classical DLW (Fig. 5,a), and the decoupled structure (Fig. 5,b) [2,7].

In the Fig. 6 the surfaces $Z_e(a,t)$, (a), and $\Psi_d(a, t)$, (b), for the SW DLW structure, λ = 10 cm, where $Z_e(a, t)$ is the value of the effective shunt impedance of the structure.

For the simple SW DLW (see Fig. 5,a) the most efficient reduction of higher harmonics (7) is achieved, [10], by enlarging the iris aperture *a*~20 mm to balance the electric and magnetic field components so that *A* ~ *-B*, Fig. 6,b. At the same time the effect of the oscillating term onto the average trajectory (11) is reduced. It leads however also to a reduction of the RF, efficiency, Fig. 6,a.

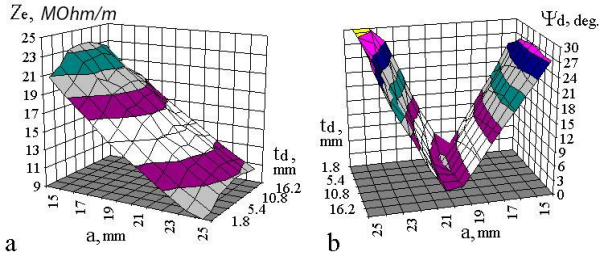

Fig. 6. The surfaces $Z_e(a,t)$ (a), and $\Psi_d(a, t)$ (b), for the SW DLW structure, λ = 10 cm

Balancing the field components while keeping a high RF efficiency requires to decouple the control of the DS RF parameters in efficiency and of the field distribution near axis, [2], which requires structure design with more degrees of freedom than the classical DLW.

Such possibility was confirmed for the TE – structure, see [7] the reference therein, and realized in [10] by changing the parameter r_w (see Fig. 5,b).

The field distributions for the optimized DLW, and two options of the decoupled structure are shown in Fig. 7. Calculated values are Z_e=15.7 MOhm/m, *B/A*=-0.8549, Ψ_{dmin}=2.39° for the DLW, Z_e=36.6 MOhm/m, *B/A*= -0.7904, Ψ_{dmin}=2.07° and Z_e=32.0 MOhm/m, *B/A*= -1.0008, Ψ_{dmin}=2.10°, for two decoupled structures, respectively.

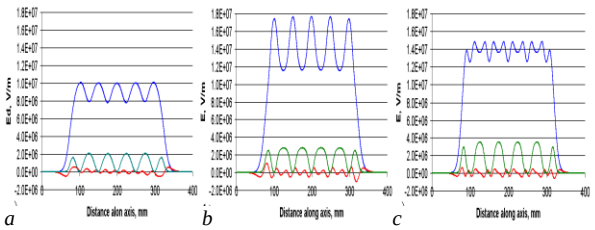

Fig. 7. The field distributions along the SW deflector axis (see Fig. 10) for the optimized DLW (a) and two options of the decoupled structure (b) and (c). Blue – E_d, ϕ=0, red – E_d, ϕ=90°; green – E_z, ϕ=90°

The beam dynamics simulations through the SW structures for the 50 MeV electron bunch shows ~ 4 times less transverse emittance growth even for not optimized DLW, a=12 mm, Z_e=26.4 MOhm/m, Ψ_{dmin} >30°, as compared to more RF effective, a=6.7 mm, Z_e=61 MOhm/m TE – structure, which has the equal phasing of the hybrid waves *HE* and *HM*. It confirms the necessity of oscillations reduction in (10). For the optimized SW DS with field distributions in Fig. 7 no emittance growth observed as compared with not optimized DLW and TE structure for 50 MeV beam.

2.3. INPUT KICK

The input/output end cells of the DS structure, both for TW and SW operating mode, with the connected beampipes deteriorate the periodicity of the structures and can cause a transverse kick of the bunch as the whole, similar to oscillating impact in (10), The field penetrating into the beampipe decays away from the cavity but provides an initial transverse kick. To reduce this part of the deflection and thus simultaneously reduce the total kick the beampipe radius should be as small as reasonably possible.

The methods for the input kick reduction are considered in [6]. For the SW DS's end cells together with the beampipe the criterion is suggested

$$Int_{1t} = \int_{-\infty}^{z} E_d(z', \phi = 90^0) dz' = 0, \qquad (11)$$

where z corresponds to the middle of the first iris. The condition (11) results in a reduced variation of *Ed*, ϕ=90° in the end cell, comparable to the residual *Ed*, ϕ=90° variation in the regular cells, and a minimized kick in the end cells. Together with reduction of oscillating impact in (1), the reduced input kick ensue bunch motion near axis, in the region with the minimal aberrations.

3. DISPERSION CURVE CORRECTION

The opposite phasing of the hybrid waves *HE* and *HM* defines a negative dispersion of the DS. For an effective aberration reduction the amplitudes should be balanced, $A \sim -B$, but this balance can be obtained only in the vicinity of the inversion point with β_g=0, θ <180°, [6], where β_g is the group of the operating wave. The inversion phenomenon is the consequence of the field distribution in the hybrid waves *HE* and *HM* even for a single passband, when mode mixing effects are absent.

Differing from the small pitch approximation, for the real DLW the value of aperture radius a for inversion β_g<0 to β_g>0, depends on θ, [6]. Together with more flexibility, the inversion phenomenon and, mainly, the dependence of the inversion point on θ provides some limitations on the DS dispersions properties.

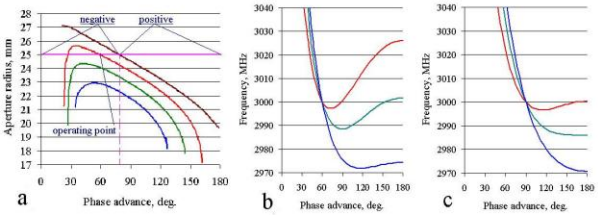

Fig. 8. The dependences of the aperture radius a on θ (a) and the dispersion curves for the DLW TW structure with θ=60° (b) and θ=120° (c) for β_g= 0.01, -0.02, -0.03, (red, green and blue curves), respectively [6]

For TW operating mode with low θ it results in not monotonous (Fig. 8,b,c), some times not acceptable shape of the dispersion curve for β_g~-0.01 (see [6] for more explanations). The low $|\beta_g|$ is required for higher RF efficiency. For SW DS with minimized aberrations it leads to a narrowed operating passband with not large frequency separation near the operating mode, [10].

To improve the deteriorated dispersion curve, we apply the resonant method, originally proposed for deflecting plane stabilization in DLW's, [11]. One resonant slot (1 in Fig. 9,a) with eigenfrequency f_s much higher than the operating frequency f_0 is introduced into the disk to interact with the modes of the operating deflection direction, differing from the original idea. The intensity of the slot excitation depends on both f_s and θ of the DS's mode. The mode frequency shift, caused by the slots, is $\delta f \sim \sin(\theta)^2/(f_s^2 - f_0^2)$, resulting in a stronger pushing down for original DS's modes with $\theta \sim 180°$. To provide a larger δf with smaller slot excitation and minimize the perturbations of the optimized field distributions in DS, slots in adjacent disks are rotated by 180°, realizing *C4* group of DS's symmetry.

In Fig. 9,b the influence of the slots on the dispersion curve for deflecting orientation is illustrated for a critical case, θ=60°, β_g~-0.01 (see the red curve in Fig. 8,b). The slot opening angle is ~320, corresponding to $f_s \sim 2f_0$. As one can see from Fig. 9,b, such slot opening results in monotonous dispersion curve for modes of deflecting directions. Simultaneously the separation in frequency with dispersion curve for modes with perpendicular field direction is obtained.

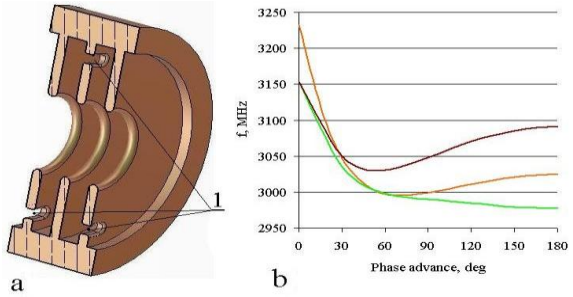

Fig. 9. The DLW DS with slots (1), θ=60°, β_g =-0.01 (a); original (red) and corrected (green) dispersion curves for deflecting polarizations and dispersion curve for perpendicular polarization (brown) after correction (b)

In simulations we do not have a significant increasing both for Ψ_d and Ψ_z values due to slots, even for such not so small opening and essential reduction of RF parameters. Definitely, smaller perturbations of the original dispersion curve can be corrected with smaller slot opening with further appropriate reduction of slots both at the field distribution and RF parameters.

For the SW DS case the slots application is considered in [10].

SUMMARY AND ACKNOWLEDGEMENTS

In this report the deflecting RF structures are considered from a new point of view – minimization as possible of intrinsic distortions in modern DS application – particle distribution transformations in the bunch. The detailed analysis of the field distribution in DS revealed the reasons of aberrations, generated by nonlinear additions in the field distribution.

The methods for selection and design of deflecting structures with a minimized level of aberrations, are developed. The examples of practical realizations of DS's combining improved field quality and a high RF efficiency, are presented.

The short SW deflector, based of the developed decoupled structure, Fig. 10, left, is now in preparation for construction in DESY, Hamburg, for precise measurements of electron beam parameters.

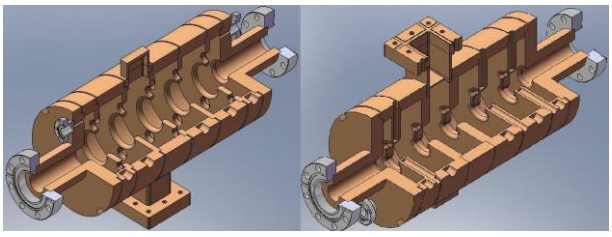

Fig. 10. SW deflectors with minimized E_d aberrations, the optimized DLW (left) and the decoupled structure (right)

This study is supported in part by the grant RBFR N12-02-00654-a.

REFERENCES

1. P. Emma et al. A transverse RF deflecting structure for bunch length diagnostics. *SLAC, LCLS-TN-00-12 (2000)* // *Proc. PAC.* 2001, p. 2353. D. Malyutin et al. Simulations of the longitudinal phase space measurements with the transverse deflecting structure at PITZ // *Proc. IPAC.* 2012, p. 637, 2012.
2. V. Paramonov. Deflecting structures with minimized level of aberrations // *Proc. Linac.* 2012, p. 445.
3. Y. Garault. Etude d'une Classe d'Ondes electromatiques Guides: Les Ondes EH / *CERN, CERN 64-43, 1964.*
4. H. Hahn. Deflecting Mode in Circular Iris-Loaded Waveguides // *Rev. Sci. Inst.* 1963, v. 34, p. 1094.
5. B.W. Montague. Radio frequency separators // *Linear Acceletors* / Ed. P. Lapostolle, E. Septier. Amsterdam, 1970.
6. V. Paramonov. Field distribution analysis in DS // *DESY 18-13, arXiv:1302.5306v1, 2013.*
7. V. Paramonov, L. Kravchuk, K. Floettmann. Parameters of a TE-type deflecting structure for the S-band frequency range // *Proc. Linac.* 2012, p. 366.
8. G.A. Loew et al. Investigations of Traveling-Wave separators for the Stanford two-mile accelerator // *The Rev. of Sci. Instr.* 1964, v. 35, №4.
9. K. Floettmann. ASTRA - A space charge tracking algorithm, http://www.desy.de/~{mpyflo}.
10. V. Paramonov, K. Floettmann, L. Kravchuk, et al. Standing wave RF deflectors with reduced aberrations // *Proc. RuPAC.* 2012, p. 590.
11. V. Paramonov, L. Kravchuk. The Resonant Method of Deflection Plane Stabilization // *Proc. Linac.* 2010, p. 434.

Article received 08.09.2013

СНИЖЕНИЕ УРОВНЯ АБЕРРАЦИЙ В ОТКЛОНЯЮЩИХ ВЧ-СТРУКТУРАХ ДЛЯ ПРЕОБРАЗОВАНИЯ РАСПРЕДЕЛЕНИЯ ЧАСТИЦ В СГУСТКЕ

В.В. Парамонов, П.В. Орлов, K. Floettmann

Проведен общий анализ распределения и сформулирован критерий выбора и разработки отклоняющих ВЧ-структур (ОС) с минимизированными нелинейными добавками (НД), обусловленными высшими гармониками НД. Рассмотрены различия, определяемые режимом работы ОС – бегущей или стоячей волны, причины увеличения уровня аберраций на отдельных участках секций ОС. Исследованы искажения дисперсионной характеристики ОС, сопутствующие уменьшению аберраций, и предложен способ коррекции этих искажений. Сформулированы ограничения на минимальный уровень аберраций в режимах бегущей и стоячей волн. Кратко приводятся примеры ОС в режимах бегущей и стоячей волн, имеющих уменьшенный, как минимум на порядок, уровень нелинейностей в распределении отклоняющего поля.

ЗНИЖЕННЯ РІВНЯ АБЕРАЦІЙ У ВІДХИЛЯЮЧИХ ВЧ-СТРУКТУРАХ ДЛЯ ПЕРЕТВОРЕННЯ РОЗПОДІЛУ ЧАСТИНОК У ЗГУСТКУ

В.В. Парамонов, П.В. Орлов, K. Floettmann

Проведено загальний аналіз розподілу і сформульовано критерій вибору і розробки відхиляючих ВЧ-структур (ВС) з мінімізованими нелінійними добавками (НД), зумовленими вищими гармоніками НД. Розглянуто відмінності, зумовлені режимом роботи ВС – хвилі, що біжить або стоїть, причини збільшення рівня аберацій на окремих ділянках секцій ВС. Досліджено спотворення дисперсійної характеристики ВС, супутні зменшення аберацій, і запропоновано спосіб корекції цих спотворень. Сформульовано обмеження на мінімальний рівень аберацій в обох режимах хвиль. Коротко наводяться приклади ВС у режимах бігучої і стоячої хвиль, які мають зменшений, як мінімум на порядок, рівень нелінійностей у розподілі відхиляючого поля.